Boise State University
ScholarWorks

CGISS Publications and Presentations

Center for Geophysical Investigation of the Shallow Subsurface (CGISS)

1-1-2006

Relating Damping to Soil Permeability

Paul Michaels
Boise State University

This is an author-produced, peer-reviewed version of this article. The final, definitive version of this document can be found online at *Journal of Geomechanics*, published by American Society of Civil Engineers. Copyright restrictions may apply. DOI: 10.1061/(ASCE)1532-3641(2006)6:3(158)

This is an author-produced, peer-reviewed version of this article. The final, definitive version of this document can be found online at International Journal of Geomechanic, published by American Society of Civil Engineers. Copyright restrictions may apply. doi: 10.1061/(ASCE)1532-3641(2006)6:3(158)

Relating Damping to Soil Permeability

Paul Michaels, PE Member ASCE

Abstract: Published comparisons of complex moduli in dry and saturated soils have shown that viscous behavior is only evident when a sufficiently massive viscous fluid (like water) is present. That is, the loss tangent is frequency dependent for water saturated specimens, but nearly frequency independent for dry samples. While the Kelvin-Voigt (KV) representation of a soil captures the general viscous behavior using a dashpot, it fails to account for the possibly separate motions of the fluid and frame (there is only a single mass element). An alternative representation which separates the two masses, water and frame, is presented here. This Kelvin-Voigt-Maxwell-Biot (KVMB) model draws on elements of the long standing linear viscoelastic models in a way that connects the viscous damping to permeability and inertial mass coupling. A mathematical mapping between the KV and KVMB representations is derived and permits continued use of the KV model, while retaining an understanding of the separate mass motions.

Introduction

The classic Kelvin-Voigt (KV) solid may be the most enduring and ubiquitous model used to represent the engineering behavior of soils. Examples of its application include compressibility and settlement (Das, 1993), as well as the response of soils under impact (Roesset et al., 1994). The model also governs the analysis of standard soil tests, including consolidation (ASTM-D2435, 1996) and resonant-column tests (ASTM-D4015, 1996). The model also finds application in describing ground water flow through unconsolidated granular soils (Domenico and Schwartz, 1990). The KV representation of a soil element places a dashpot, c, in parallel with the spring, k (see Fig. 1a). This system, composed from a single element, is a single degree of freedom oscillator, and

[1]Associate Professor, Boise State University, 1910 University Drive, Boise, Idaho 83725, Email: pm@cgiss.boisestate.edu

This is an author-produced, peer-reviewed version of this article. The final, definitive version of this document can be found online at International Journal of Geomechanic, published by American Society of Civil Engineers. Copyright restrictions may apply. doi: 10.1061/(ASCE)1532-3641(2006)6:3(158)

this is the basis for the analysis of the resonant column test. If this single degree of freedom element is joined with other similar elements, the result is a multi-degree of freedom system (Fig. 1b). When enough elements are cascaded, the assemblage can represent the 1-D propagation of an SH-wave.

A number of authors have represented the dashpot-spring combination in terms of other tractable components. In extending Terzaghi's original one-dimensional theory of consolidation to three dimensions, Biot (1941) makes reference to Terzaghi's rubber sponge analogy as a way to describe the response of a saturated soil to compression. Later, Biot's papers on wave propagation introduce the idea of a representing the pores by small cylinders. The cylinder diameter became the key parameter needed to quantify permeability (Biot, 1956a). Biot used the cylinder diameter to extend his theory to include turbulent flow beyond a defined transition frequency (Biot, 1956b). Biot's later work includes a number of figures which represent the spring and dashpot in terms of frame stiffness and fluid-frame viscous damping. Examples may be found in Biot (1962b) and Biot (1962a). Similar descriptions can also be found in Gassmann (1951) with his "open" and "closed" systems being end members of permeable and impermeable cases. The choice of uniform, spherical grains (Gassmann, 1951), or cylindrical pores of the same uniform diameter (Biot, 1956a) fall short of describing actual soils. Their value is in that such simplifications lead to a tractable analysis. For example, the capillary tube models of fluid flow through soils have been used to derive Darcy's law (Bear, 1972).

In early resonant column studies, dry samples were evaluated (Hardin, 1965) . The resulting measurements were in conflict with the constant viscosity property of the KV model. In order to retain a viscous representation, an effective viscosity was proposed which varied inversely with frequency. This introduction of an "effective" viscosity has become wide spread and integrated into engineering practice (Kramer, 1996). The continued use of the concept is testimony to the strong appeal of the KV representation, even in cases where a viscous effect is not observed. Stoll (1985), demonstrated that the introduction of water into the pore spaces could lead to a classic viscous response, suggesting that a dense viscous fluid, such as water, is required. Stoll presented results on an Ottawa sand which demonstrated an increase in damping with frequency, but only for water saturated samples. In the case of dry samples, damping remained constant with frequency.

This is an author-produced, peer-reviewed version of this article. The final, definitive version of this document can be found online at International Journal of Geomechanic, published by American Society of Civil Engineers. Copyright restrictions may apply. doi: 10.1061/(ASCE)1532-3641(2006)6:3(158)

Inspired by Stoll's reports for saturated soil and the theoretical foundation of Biot (1962a), the author formulated the KVMB model. This model behaves very much like the KV model, but splits the mass into two parts, and is a re-arrangement of the elements in series (similar to a Maxwell body). When relating this KVMB model to a saturated soil, porosity can be used to define the mass ratio (frame to pore fluid). The dashpot is an expression of the permeability which controls the relative motion between frame and pore fluid. Further, it is possible to mathematically map the KVMB model elements to those of the classic KV representation, and thus relate determinations of porosity and KV viscous damping to permeability.

The KVMB Representation

A major limitation of the KV model is that the mass is treated as a single element. A two phase medium, like a saturated soil, can not be fully represented with the masses bundled in this way. The KVMB representation presented here separates the mass into pore fluid and solid frame components (according to porosity). Viscous damping is then due to the frictional losses resulting from the relative motion between fluid and frame. Frictional losses from this motion produces the "dashpot". The KVMB dashpot depends on permeability.

The KVMB elemental representation is shown in Figure 2a. As in the case of the classic KV model, there is a single dashpot and a single spring, but arranged in series (reminiscent of the Maxwell model). Also, we can view the system from either point of view, an oscillator (single element) or wave (assemblage of elements). The significant difference is the explicit separation of the water mass from the frame mass by the dashpot (Biot's influence). The dashpot controls the relative motion between the two mass components (fluid and frame), and this permits us to relate the dashpot to permeability.

Dampened Oscillator Points of View

Engineering practice has a significant investment in the KV model. Our very concept of viscous damping and damping ratio for an oscillator are uniquely bound to this single degree of freedom (SDOF) system. Therefore, it is useful to find a mathematical mapping between the KV and KVMB representations. Both models produce very similar behavior, but the KVMB model can

This is an author-produced, peer-reviewed version of this article. The final, definitive version of this document can be found online at International Journal of Geomechanic, published by American Society of Civil Engineers. Copyright restrictions may apply. doi: 10.1061/(ASCE)1532-3641(2006)6:3(158)

relate that behavior to soil fluid-frame interaction in a more direct way. A mapping between the KV and the KVMB models can be achieved through a *Gedanken Versuch* (thought experiment). This is done by examining a single dampened oscillator element for both representations. The components are considered matched when the free response time histories are as close as possible. We consider the free response due to an initial condition consisting of a velocity impulse applied to either the frame mass (KVMB), or the single mass element (KV). The mapping is facilitated by decoupling the differential equations and relating two of the respective eigenvalues. Thus, it is possible to compute an equivalent KV dashpot from the permeability and degree of inertial mass coupling represented by the KVMB model.

Decoupling the KV Representation

The governing differential equation for the free response of the KV model corresponds to the well understood SDOF system,

$$m\ddot{u} + c\dot{u} + ku = 0 \quad , \tag{1}$$

where mass motion is given by displacement, u, velocity, $\dot{u}$, and acceleration, $\ddot{u}$. This second order ordinary differential equation (ODE) can be recast as a coupled system of two first order ODE's (Sadun, 2001),

$$\frac{d}{dt}\mathbf{u} = \mathbf{A_{kv}} \cdot \mathbf{u} \tag{2}$$

$$\frac{d}{dt}\mathbf{u} = \frac{d}{dt}\begin{bmatrix} u \\ \dot{u} \end{bmatrix} = \begin{bmatrix} 0 & 1 \\ -\frac{k}{m} & -\frac{c}{m} \end{bmatrix} \cdot \begin{bmatrix} u \\ \dot{u} \end{bmatrix} \quad , \tag{3}$$

where $\mathbf{u}$ is the displacement-velocity vector. In this autonomous form, we recognize an eigenvalue problem which can be diagonalized in a new basis given by the eigenvectors of matrix, $\mathbf{A_{kv}}$. Equations 1 and 3 are equivalent, as are their solutions. In the specific case of an under-damped system, the solution is an exponentially decaying sinusoid. The eigenvalues of $\mathbf{A_{kv}}$ are complex, the imaginary part giving the damped oscillation frequency, and the real part the exponential decay envelope of the solution. The analytic solution to equation 3 is given as (Sadun, 2001),

$$\begin{bmatrix} u(t) \\ \dot{u}(t) \end{bmatrix} = \mathbf{B_{kv}} \cdot \begin{bmatrix} e^{\lambda_1 t} & 0 \\ 0 & e^{\lambda_2 t} \end{bmatrix} \cdot \mathbf{B_{kv}^{-1}} \cdot \begin{bmatrix} u(0) \\ \dot{u}(0) \end{bmatrix} \quad , \tag{4}$$

This is an author-produced, peer-reviewed version of this article. The final, definitive version of this document can be found online at International Journal of Geomechanic, published by American Society of Civil Engineers. Copyright restrictions may apply. doi: 10.1061/(ASCE)1532-3641(2006)6:3(158)

where the new, diagonalized basis is given by matrix, $\mathbf{B_{kv}}$, the columns of which are the eigenvectors of $\mathbf{A_{kv}}$. For our particular choice, the initial conditions are given by $u(0) = 0$ and $\dot{u}(0) = 1$. In the under-damped case, the eigenvalues λ_i will be complex conjugates.

Decoupling the KVMB Representation

By similar reasoning, the KVMB model shown in Figure 2a obeys the coupled governing differential equation,

$$\frac{d}{dt}\mathbf{u} = \mathbf{A_{kvmb}} \cdot \mathbf{u} \tag{5}$$

$$\frac{d}{dt}\begin{bmatrix} u_f \\ \dot{u}_f \\ \dot{u}_w \end{bmatrix} = \begin{bmatrix} 0 & 1 & 0 \\ -\frac{k}{M_f} & -\frac{d}{M_f} & +\frac{d}{M_f} \\ 0 & +\frac{d}{M_w} & -\frac{d}{M_w} \end{bmatrix} \cdot \begin{bmatrix} u_f \\ \dot{u}_f \\ \dot{u}_w \end{bmatrix} \quad , \tag{6}$$

where u_f is the frame-mass displacement, $\dot{u}_f$ is the frame-mass velocity, and $\dot{u}_w$ is the water-mass velocity. This 2DOF system is 3x3 with 3 eigenvalues. The solution giving the free response of the KVMB system to initial conditions is,

$$\begin{bmatrix} u_f(t) \\ \dot{u}_f(t) \\ \dot{u}_w(t) \end{bmatrix} = \mathbf{B_{kvmb}} \cdot \begin{bmatrix} e^{\gamma_1 t} & 0 & 0 \\ 0 & e^{\gamma_2 t} & 0 \\ 0 & 0 & e^{\gamma_3 t} \end{bmatrix} \cdot \mathbf{B^{-1}_{kvmb}} \cdot \begin{bmatrix} u_f(0) \\ \dot{u}_f(0) \\ \dot{u}_w(0) \end{bmatrix} \quad , \tag{7}$$

where there are 3 eigenvalues, γ_i , and the columns of the new basis matrix, $\mathbf{B_{kvmb}}$, are the eigenvectors of $\mathbf{A_{kvmb}}$. Our choice of initial conditions is $u_f(0) = 0$, $\dot{u}_f(0) = 1$, and $\dot{u}_w(0) = 0$. In both the KV and KVMB cases, the single mass, or the frame-mass receives an initial velocity impulse respectively. For an under-damped system, equation 7 is an exponentially decaying sinusoid superimposed on an exponentially decaying trend. This superimposed trend is small in amplitude, and thus the two models can be effectively mapped.

Motivation for Mapping KV to KVMB

The advantage of the KVMB system lies in its separation of the two mass components, solid and water. Once the masses are separated, the viscous damping may be related to the permeability. Motivation for the mapping resides in the existing laboratory and field methods which are grounded

This is an author-produced, peer-reviewed version of this article. The final, definitive version of this document can be found online at International Journal of Geomechanic, published by American Society of Civil Engineers. Copyright restrictions may apply. doi: 10.1061/(ASCE)1532-3641(2006)6:3(158)

in the KV model. We can relate the laboratory or field measured spring and dashpot values (KV model) to corresponding values for the KVMB spring and dashpot. Assuming porosity is known, the resultant KVMB dashpot can be related to the soil permeability, producing a technique to evaluate permeability from either resonant column or SH-wave determinations of damping (Michaels, 1998).

An intuitive description of the mapping is as follows. At one end limit, say in a clay, the pore fluids move largely with the frame, the lack of significant relative motion leading to small damping values. We say that the masses are coupled in a clay, and the KVMB dashpot would have a large value (but the KV dashpot would be small in value). At the other extreme, say a gravel with large pores, the pore fluids and frame move independently. We say that the masses are uncoupled in a gravel, and the KVMB dashpot has a small value (as does the KV dashpot). The frictional losses are small due to the large pore diameters.

Between these two extremes, say for a sand, the permeability is small enough to maximize viscous friction and hence damping. That is, the pores are large enough to permit significant relative motion between the pore fluid and frame, but small enough to lead to significant viscous friction and damping. Intuitively, we expect a peak in equivalent KV damping value to occur at the transition between coupled and uncoupled cases.

Experimental support for the view that viscous damping is related to fluid-frame interaction in sands is found in Stoll (1985). Stoll demonstrated that resonant column testing of saturated sands produces a frequency dependent damping, while dry samples produce a damping which is nearly frequency independent. In short, water can produce a larger viscous damping effect than air since the mass of water will be more than the mass of air for the same pore volume. Thus, when combined with porosity and pore fluid specifications, the KVMB representation is able to predict both the large and small viscous effects corresponding to saturated and dry conditions respectively.

Mapping KV and KVMB Representations

As previously mentioned, the mapping is done through the thought experiment. Each dampened oscillator, KV and KVMB, is excited by a velocity impulse applied to the combined or frame mass respectively. We consider the spring and dashpot components of the two alternative models mapped

This is an author-produced, peer-reviewed version of this article. The final, definitive version of this document can be found online at International Journal of Geomechanic, published by American Society of Civil Engineers. Copyright restrictions may apply. doi: 10.1061/(ASCE)1532-3641(2006)6:3(158)

when the resultant free response of the frame mass (KVMB) is as close as possible to the response of the combined mass (KV). We can view the response of each system as a time series describing the position of the mass as a function of time. For the KVMB model, this would be the frame mass, for the KV model the combined mass.

A scalar metric which quantifies the similarity between these two displacement signals is given by the angle between the two time series. The angle is

$$\theta = \arccos\left(\frac{u_f^T \cdot u}{\|u_f\| \cdot \|u\|}\right) \quad , \tag{8}$$

where u_f is the displacement time history of the solid frame mass of the KVMB model, and u is the displacement of the combined mass in the KV model. The denominator terms are the euclidean (L2) norms for the two signals. Because both signals are essentially exponentially decaying sinusoids, there is no need to consider the response beyond the point where the motion has died out. The angle θ provides a scalar metric which can be used to evaluate the mapping between the two representations. The smaller the value of θ, the better the match. Thus, if the two time histories were identical, the angle would be zero. In the author's experience, values of θ less than 5 degrees correspond to time histories which are virtually indistinguishable.

The solution is to discard the purely real eigenvalue of the KVMB system, and retain only the complex-conjugate eigenvalue pair. It is the complex-conjugate pair which produce that part of the response associated with the KV model. The retained KVMB eigenvalues are substituted into the KV solution which gives the eigenvalues in terms of the spring and dashpot constants. One simply back solves for the component values from the eigenvalues. The solution is to set $\lambda_1 = \gamma_1$, $\lambda_2 = \gamma_2$, discard γ_3, and

$$\frac{k}{m} = \lambda_1 \cdot \lambda_2 \quad , \tag{9}$$

$$\frac{c}{m} = -\left(\lambda_1 + \lambda_2\right) \quad , \tag{10}$$

where γ_1 and γ_2 are the retained complex conjugate eigenvalues from the KVMB representation, and m is the KV mass which effectively completes the mapping. Thus, it is not necessary to actually compute the time series contemplated in the thought experiment. We need only determine the KVMB eigenvalues to compute the effective spring-mass and dashpot-mass ratios of the KV

This is an author-produced, peer-reviewed version of this article. The final, definitive version of this document can be found online at International Journal of Geomechanic, published by American Society of Civil Engineers. Copyright restrictions may apply. doi: 10.1061/(ASCE)1532-3641(2006)6:3(158)

system. Note that we obtain only ratios with respect to mass on the left hand side, not individual values for the the spring and dashpot. It is these ratios that determine the eigenvalues of the KV system given in equation 3.

Figure 3 illustrates the mapping for a specific KVMB oscillator. Here, values of frame mass (1000 kg) and frame spring (1E+8 N/m) were held constant while the KVMB dashpot value varied over a range from 10 to 10^9kg/s. Two cases of water mass are shown and indicated by the ratio of frame to fluid masses. The case where the water and frame masses are equal is shown as a solid curve.

Figure 3a shows the mapped equivalent dashpot for the KV model. At low values of damping, the KV and KVMB dashpots are equal (similar to what we would expect for a very permeable soil, like a gravel). The equivalent spring stiffness is shown in Figure 3b. The KVMB and KV stiffness values are also equal at low KVMB damping values. As the KVMB damping value increases, we reach a peak in the effective KV dashpot. This marks the transition point where the water and the frame begin to move together. Beyond the peak, the motion becomes increasingly coupled, and due to the reduced relative motion between frame and water, we have less friction and less equivalent damping. In terms of a soil, a large KVMB damping would represent a clay or other soil of low permeability. The water, being dragged in the pores, reduces the frictional losses. Further, with the two masses largely moving together, we expect a reduction in the resonant frequency of the moving frame. This predicted reduction in natural frequency is expressed as an apparent reduction in the KV stiffness (since the frame mass is constant). In this example, the natural frequency of the oscillator drops from about 50 Hz to 35 Hz.

Normalization to Damping Ratio

While the above example is for a specific mass, spring and dashpot, we can view the problem from a normalized, general point of view. We do this by modifying the damping plot shown in Figure 3a, replacing damping values with damping ratios. There are two damping ratios to be considered (KV and KVMB). Although the formulas are identical, the ratios correspond to different arrangements of the elements. The formula for damping ratio is well known, and is given

This is an author-produced, peer-reviewed version of this article. The final, definitive version of this document can be found online at International Journal of Geomechanic, published by American Society of Civil Engineers. Copyright restrictions may apply. doi: 10.1061/(ASCE)1532-3641(2006)6:3(158)

by

$$\xi = \frac{C}{2\sqrt{K \cdot M}} \quad , \tag{11}$$

where C is the dashpot's viscous damping (kg/s), K is spring's stiffness (N/m), and M is mass (kg). Damping ratio, ξ, is unitless. The dashpot and spring require no comment for either the KV or KVMB models. The mass does require some thought, since there are two of them in one model, and one mass in the other. Since the left hand side of equations 9 and 10 are ratios, we can eliminate the mass in computing the equivalent KV damping ratio of equation (11). The resulting expression for the KV damping ratio in terms of the complex conjugate eigenvalues taken from the KVMB system is

$$\xi = \frac{\sqrt{(\lambda_1 + \lambda_2)^2}}{2\sqrt{\lambda_1 \lambda_2}} = \frac{|\lambda_1 + \lambda_2|}{2\sqrt{\lambda_1 \lambda_2}} \quad . \tag{12}$$

On the other hand, there is no single correct answer for which KVMB mass to employ in equation (11). Two choices are the sum of the water and frame masses, or the frame mass alone. The former makes sense for coupled motion, the later for uncoupled. Fortunately, for porosities likely to be encountered in most soils, the difference between these two options will be small. In this paper, the combined mass of water plus frame has been used to compute the KVMB damping ratio.

Figure 4 shows the equivalent KV damping ratio as a function of the KVMB damping ratio. Curves are shown for different mass ratios between the frame and water. Note that as the fluid mass declines (larger mass ratio), the curve maximum shifts down and to the left. A decrease in mass ratio would correspond to a decline in porosity for a soil. It also suggests that replacing water with a less dense fluid (say air) will produce less viscous damping.

In the next section, the KVMB dashpot will be related to damping in the manner which Biot approached the problem, a capillary tube soil model. The partitioning of the frame and water masses will be based on porosity and the assumption of a saturated soil. The development is focused on describing shear motion and shear waves (not compressional waves).

This is an author-produced, peer-reviewed version of this article. The final, definitive version of this document can be found online at International Journal of Geomechanic, published by American Society of Civil Engineers. Copyright restrictions may apply. doi: 10.1061/(ASCE)1532-3641(2006)6:3(158)

Relating KVMB Damping to Permeability

We follow the model proposed by Biot (1956a) in his work on wave propagation. A pore is represented by a right-circular cylinder of diameter, δ . The head loss, h_f , for fluid flow in the pore is then given by the Darcy-Weisbach equation,

$$h_f = \frac{fLv_s^2}{2\delta g} \quad , \tag{13}$$

where L is the pore length, v_s is the specific flow velocity in the pore, g is the acceleration due to gravity, and f a friction factor. We follow Biot's example, and assume laminar flow. Thus, we let the friction factor be given in the usual way,

$$f = \frac{64}{R_e} = \frac{64\mu}{\rho_w \delta v_s} \quad , \tag{14}$$

where $\mathsf{R_e}$ is the Reynolds number, ρ_w the pore fluid density, and μ is the pore fluid dynamic viscosity (units of $Pa \cdot s$). Substituting equation 14 into equation 13 we have

$$h_f = \frac{32\mu L v_s}{\rho_w \delta^2 g} \quad . \tag{15}$$

For an elemental volume of soil represented by a solid perforated by uniform, parallel, cylindrical pores, the net flow velocity out of a cross-section including many pores is

$$v = n v_s \quad , \tag{16}$$

where n is the porosity for the given volume. For our element of length L , and cross-sectional area, A , Darcy's equation is given by

$$\frac{Q}{A} = v = K_d \left(\frac{h_f}{L} \right) \quad , \tag{17}$$

where Q is the volumetric flow rate, K_d is the hydraulic conductivity (units of m/s) . Equating the velocities, v , in equations 16 and 17, we can solve for hydraulic conductivity in terms of pore size and the other model parameters,

$$K_d = \frac{n\rho_w \delta^2 g}{32\mu} \quad . \tag{18}$$

This result is the same as that given by Bear (1972) (see p. 165). Bear make the point that the 32 in the denominator is "meaningless", and that some authors scale the 32 by a "tortuosity" factor

This is an author-produced, peer-reviewed version of this article. The final, definitive version of this document can be found online at International Journal of Geomechanic, published by American Society of Civil Engineers. Copyright restrictions may apply. doi: 10.1061/(ASCE)1532-3641(2006)6:3(158)

which scales the representation to a real soil in which the pores are not parallel or cylindrical, and a diverse size of pores exist. This last point leads one to conclude that δ is meant to be an "effective" pore diameter, representative of the actual pore diameters. Essentially, multiplying 32 by a tortuosity only affects the relationship between K_d and δ .

Biot (1956a) gives a dissipation coefficient in his equation (6.8),

$$b = \frac{\mu n^2}{\overline{k}} \quad , \tag{19}$$

where we have used the current notation for porosity. Biot refers to $\overline{k}$ as Darcy's coefficient of permeability. This is in fact the absolute permeability (units of m^2), and is related to our hydraulic conductivity by

$$\overline{k} = \frac{K_d \mu}{g \rho_w} \quad . \tag{20}$$

Further, Biot's equation (7.11) gives b for cylindrical pores as

$$b = \frac{32 \mu n}{\delta^2} \quad . \tag{21}$$

If we substitute equation 20 into 19, we obtain

$$b = \frac{n^2 g \rho_w}{K_d} \quad . \tag{22}$$

Substituting K_d from equation 18 into 22 , we obtain equation 21, thus illustrating that our K_d of equation 18 is in exact agreement with Biot's paper, and his assumptions at low frequencies and laminar flow.

Biot's dissipation factor, b, is the coefficient of a term in his wave equation (6.7). That is, b is the coefficient of the term which is the difference between the fluid and frame velocities. Thus, b plays the role of a dashpot connected between the frame and water masses of our Figure 2a. It is not, however, the lumped dashpot value. We note that b has units of kg/s per m^3, while an ideal dashpot element has units of kg/s . Biot's damping coefficient is to a dashpot damping value as density is to mass. To obtain the ideal, lumped, components (spring, dashpot, and mass), we need to integrate the specific properties over a common volume of material being represented.

This is an author-produced, peer-reviewed version of this article. The final, definitive version of this document can be found online at International Journal of Geomechanic, published by American Society of Civil Engineers. Copyright restrictions may apply. doi: 10.1061/(ASCE)1532-3641(2006)6:3(158)

Determining Spring, Mass, and Dashpot for a Volume

Consider an elemental volume of cross-sectional area, A , and length, L , as shown in Figure 5. For a simple shear due to a traction F/A , and a frame material with shear modulus, G_f, we have

$$G_f = \frac{\left(\frac{F}{A}\right)}{\left(\frac{\Delta x}{L}\right)} = \frac{\left(\frac{k\Delta x}{A}\right)}{\left(\frac{\Delta x}{L}\right)} = \frac{kL}{A} \quad . \tag{23}$$

Solving for the spring constant, we have

$$k = \frac{G_f A}{L} \quad . \tag{24}$$

For our KVMB dashpot, we have

$$d = bAL = \left(\frac{n^2 g \rho_w}{K_d}\right)(AL) \quad . \tag{25}$$

The frame and water masses follow from porosity and the specific gravity of the solid, G_s. They are respectively,

$$m_f = AL\,(1-n)\,G_s \rho_w \tag{26}$$

$$m_w = nAL\rho_w \quad . \tag{27}$$

KV Damping Ratio vs Hydraulic Conductivity

Figure 6 illustrates the mapping at a single frequency, 50 Hz. In this thought experiment, we consider a single element of soil with length L. For a desired natural frequency, ω, we can determine the length of the required volume, L, stiffness-mass ratio as follows:

$$L^2 = \frac{G_f}{\omega^2\,(1-n)\,G_s \rho_w} \quad , \tag{28}$$

where frequency, ω , is in radians per second. We can obtain the hydraulic conductivity by solving equation (25) for K_d ,

$$K_d = \frac{n^2 g \rho_w AL}{d} \quad , \tag{29}$$

where the dashpot value, d, is varied over a range of values to produce Figure 6. Curves are computed for selected porosity values of 10, 30, and 50 percent.

This is an author-produced, peer-reviewed version of this article. The final, definitive version of this document can be found online at International Journal of Geomechanic, published by American Society of Civil Engineers. Copyright restrictions may apply. doi: 10.1061/(ASCE)1532-3641(2006)6:3(158)

To emphasize the fact that two different coupling conditions may result in the same KV damping ratio, three points have been annotated in Figure 6. Point A corresponds to maximum damping obtainable for a porosity of 30%. Point B corresponds to a largely coupled condition, and point C to a largely uncoupled condition which produce the same value of equivalent KV damping ratio ($\xi = 0.0135$).

Figure 7 gives the corresponding particle velocity time histories for the fluid and frame motions for the three cases indicated by A, B, and C in Figure 6. For the point B case ($K_d = 0.002\, m/s$), the motions are closely coupled, and the particle velocities are almost together. The slight difference in velocity between frame and water results in an equivalent KV damping ratio of 0.0135. At the other extreme, case C, there is a significant difference in the frame and mass velocities. However, the equivalent KV damping ratio is only 0.0135 since the hydraulic conductivity is large ($K_d = .06\, m/s$). The point is that the combined larger velocity difference and larger effective pore diameter in case C results in the same frictional loss that results from smaller pore diameters with less relative velocity between fluid and frame. The maximum damping occurs at point A ($K_d = .0109\, m/s$), where the combined pore diameter and relative velocity difference produce a maximum in the viscous friction.

For the three cases shown in Figure 7, the equation (8) metric was computed to assess the match between the KV and KVMB displacement time histories. The largest difference (poorest match) was for point A, and resulted in an angle of $\theta = 2.04^o$. If the two displacement time histories were to be plotted here, they would appear as one, making this an acceptable match. The best match was for point C ($\theta = .036^o$). Point B matched with a metric of $\theta = 1.47^o$.

KV Damping Ratio vs Frequency

This final example illustrates the effect of frequency on the KV damping ratio. In this thought experiment, the porosity is held at 30%. The sample length was varied to produce a range of natural frequencies for the vibrating soil element.

Figure 8 shows the equivalent KV damping ratio as a function of natural frequency for three cases of hydraulic conductivity ($0.002,\ .0109,\ .060\, m/s$ corresponding to B, A, and C of Figure 6). At 50 Hz, points B and C plot at the same point, the intersection of the $K_d = .06$ and

This is an author-produced, peer-reviewed version of this article. The final, definitive version of this document can be found online at International Journal of Geomechanic, published by American Society of Civil Engineers. Copyright restrictions may apply. doi: 10.1061/(ASCE)1532-3641(2006)6:3(158)

$K_d = 0.002\, m/s$ curves. Points B and C produce the same damping, but for the different reasons explained in the previous section (B is largely coupled, C is largely uncoupled motion between fluid and frame). Figure 8 is simply another way of looking at the same situation. What is different in this view is the effect of frequency on the equivalent KV damping ratio. The theory predicts that at low frequencies (left of a curve's apex), the motion between fluid and frame is largely coupled. At high frequencies (right of a curve's apex), the motion is largely uncoupled. A crude analogy would be to consider a table with dishes resting on a table cloth. The largely uncoupled, high-frequency case is analogous to a waiter snapping the table cloth off a table without disturbing the dishes (large relative motion between table cloth and dishes). The largely coupled, low-frequency case is analogous to slowly pulling on the table cloth. The dishes would be dragged along with the table cloth.

Conclusions

The Kelvin-Voigt (KV) model is widely employed in soil dynamics, consolidation theory, and ground water flow. While the KV dashpot represents the viscous interaction of pore fluids with frame, there is no allowance for separate motion between the fluid in frame (the masses are considered to be lumped together as a single unit). The KVMB model presented here permits the fluid and frame masses to have independent motion, and relates the dashpot connecting them to soil permeability. The two models (KV and KVMB) have been mapped through the eigenvalues of the decoupled differential equations, permitting the continued use of the KV model to be related to the KVMB and soil permeability (provided that porosity or void ratio is known).

The theory predicts the following:

- For a given porosity, there will be a maximum KV damping (point A in Figures 6 or 8). This is the point where the difference between KV and KVMB representations is largest, but always acceptable ($\theta \leq 5^o$). It is the point where the combination of significant relative motion between fluid in frame combines with a medium pore size to maximize equivalent KV damping.

- Below point A, there will be two theoretical cases which produce the same KV damping.

This is an author-produced, peer-reviewed version of this article. The final, definitive version of this document can be found online at International Journal of Geomechanic, published by American Society of Civil Engineers. Copyright restrictions may apply. doi: 10.1061/(ASCE)1532-3641(2006)6:3(158)

One is a largely coupled condition (small pores, small relative velocity between frame and fluid), and the other is a largely uncoupled condition (large pores, larger relative velocity between frame and fluid). See points B and C of Figure 6 for example.

- At low frequencies, to the left of the KV damping ratio apex, the motion will be largely coupled.
- At high frequencies, to the right of the KV damping ratio apex, the motion will be largely uncoupled.

Acknowledgments

This work is supported by U.S. Army Research Office grant DAAH04-96-1-0318. Any opinions, findings, and conclusions expressed in this material are those of the author, and do not necessarily reflect the views of the U.S. Army.

Notation

The following symbols are used in this paper.

A= cross-sectional area of soil element in thought experiment (m^2).

b= Biot dissipation coefficient $\left(\frac{kg}{s \cdot m^3}\right)$.

c = dashpot constant for KV model $\left(\frac{kg}{s}\right)$.

d = dashpot constant for KVMB model $\left(\frac{kg}{s}\right)$.

f = friction factor in a cylindrical pore (unitless).

f_n= natural cyclic frequency of soil element (Hz).

G_f = shear modulus of frame (Pa).

G_s = specific gravity of soil solids (unitless).

g = acceleration due to gravity $\left(9.81\ \frac{m}{s^2}\right)$.

h_f = head loss in a cylindrical pore (m).

K_d = hydraulic conductivity $\left(\frac{cm}{s}\right)$.

k = KV spring $\left(\frac{N}{m}\right)$.

$\overline{k}$ = absolute permeability (m^2).

k_f = spring constant of frame $\left(\frac{N}{m}\right)$.

This is an author-produced, peer-reviewed version of this article. The final, definitive version of this document can be found online at International Journal of Geomechanic, published by American Society of Civil Engineers. Copyright restrictions may apply. doi: 10.1061/(ASCE)1532-3641(2006)6:3(158)

L= length of soil element in thought experiment (m).

m= KV mass (kg).

m_f= frame mass for KVMB model(kg).

m_w= water mass for KVMB model (kg).

n = porosity (unitless).

$\mathsf{R_e}$ = Reynolds number for flow in a cylindrical pore (unitless).

t = time (s).

u = particle displacement of KV mass (m).

$\dot{u}$= particle velocity of KV mass $\left(\frac{m}{s}\right)$.

u_f= particle displacement of frame in thought experiment (m).

$\dot{u_f}$= particle velocity of frame in thought experiment $\left(\frac{m}{s}\right)$.

$\dot{u_w}$= particle velocity of water in thought experiment $\left(\frac{m}{s}\right)$.

v= net flow velocity of fluids in a cross-section of pores (m/s).

v_s= specific flow velocity in a pore (m/s).

$\gamma_1,\ \gamma_2,\ \gamma_3$= eigenvalues of KVMB representation.

δ= pore diameter (m).

$\lambda_1,\ \lambda_2$= eigenvalues of KV representation (complex conjugate pair of the KVMB).

μ = absolute viscosity of pore fluids $(Pa \cdot s)$.

ξ= damping ratio (unitless).

ρ_f = mass density of frame$\left(\frac{kg}{m^3}\right)$.

ρ_w= mass density of water $\left(1000\ \frac{kg}{m^3}\right)$.

$\omega_n = 2\pi f_n$ natural frequency of soil element in thought experiment $\left(\frac{rad}{s}\right)$.

This is an author-produced, peer-reviewed version of this article. The final, definitive version of this document can be found online at International Journal of Geomechanic, published by American Society of Civil Engineers. Copyright restrictions may apply. doi: 10.1061/(ASCE)1532-3641(2006)6:3(158)

Figure Captions

Fig. 01: Kelvin-Voigt (KV) soil representation for (a) vibrator and (b) wave assemblage.

Fig. 02: Kelvin-Voigt-Maxwell-Biot soil representation for (a) vibrator and (b) wave assemblage.

Fig. 03: Equivalent KV (a) damping and (b) stiffness for a KVMB thought experiment.

Fig. 04: Equivalent KV damping ratio as a function of KVMB damping ratio for different mass ratios.

Fig. 05: Determining a lumped spring stiffness from a soil element's shear modulus, G_f.

Fig. 06: Equivalent KV damping ratio as a function of hydraulic conductivity at 50 Hz for different porosities.

Fig. 07: Frame and water time histories corresponding to points A, B, and C of figure 6.

Fig. 08: Equivalent KV damping ratio as a function of natural frequency for a porosity of 30% for different hydraulic conductivities corresponding to points A, B, and C of figure 6.

.

This is an author-produced, peer-reviewed version of this article. The final, definitive version of this document can be found online at International Journal of Geomechanic, published by American Society of Civil Engineers. Copyright restrictions may apply. doi: 10.1061/(ASCE)1532-3641(2006)6:3(158)

References

American Society for Testing and Materials (ASTM). (1996). "Standard test method for one-dimensional consolidation properties of soils", D2435, West Conshohocken, Pa.

American Society for Testing and Materials (ASTM). (1996). "Standard test methods for modulus and damping of soils by the resonant-column method", D4015, West Conshohocken, Pa.

Bear, J., (1972). *Dynamics of fluids in porous media*, Dover, New York.

Biot, M., (1941). "General theory of three-dimensional consolidation", *J. Applied Phys.*, 12(2), 155–164.

Biot, M., (1956a). "Theory of propagation of elastic waves in a fluid-saturated porous solid. I Low-frequency range", *J. Acoustical Soc. Am.*, 28(2), 168–178.

Biot, M., (1956b). "Theory of propagation of elastic waves in a fluid-saturated porous solid. II High-frequency range", *J. Acoustical Soc. Am.*, 28(2), 179–191.

Biot, M., (1962a). "Generalized theory of acoustic propagation in porous dissipative media", *J. Acoustical Soc. Am.*, 34(9), 1254–1264.

Biot, M., (1962b). "Mechanics of deformation and acoustic propagation in porous media", *J. of Applied Physics*, 33(4), 1482–1498.

Das, B., (1993). *Principles of Geotechnical Engineering*, 3rd edition, PWS Publishing Co., Boston.

Domenico, P., and Schwartz, F., (1990). *Physical and Chemical Hydrogeology*, John Wiley & Sons, New York.

Gassmann, F., (1951). "Über die Elastizität poröser medien" *Vierteljahrsschrift der Naturforschenden Gessellschaft in Zürich*, 96, 1–23.

Hardin, B. O., (1965). "The nature of damping in sands", *Journal of Soil Mechanics, Foundations Div.*, ASCE, 91(SM1), 63–97.

Kramer, S., (1996). *Geotechnical Earthquake Engineering*, 1st edition, Prentice Hall, New Jersey.

Michaels, P., (1998). "In situ determination of soil stiffness and damping", *Journal of Geotechnical and Geoenvironmental Engineering*, 124(8), 709–719.

Roesset, J., Kausel, E., Cuellar, V., Monte, J., and Valerio, J., (1994). "Impact of weight falling onto the ground", *Journal of Geotechnical and Geoenvironmental Engineering*, 120(8), 1394–1412.

This is an author-produced, peer-reviewed version of this article. The final, definitive version of this document can be found online at International Journal of Geomechanic, published by American Society of Civil Engineers. Copyright restrictions may apply. doi: 10.1061/(ASCE)1532-3641(2006)6:3(158)

Sadun, L., (2001). *Applied linear algebra: The decoupling principle*, Prentice Hall, New Jersey.

Stoll, R., (1985). "Computer-aided studies of complex soil moduli ", *Proc., Measurement and use of shear wave velocity for evaluating dynamic soil properties*, ASCE, Reston, Va., 18–33.

This is an author-produced, peer-reviewed version of this article. The final, definitive version of this document can be found online at International Journal of Geomechanic, published by American Society of Civil Engineers. Copyright restrictions may apply. doi: 10.1061/(ASCE)1532-3641(2006)6:3(158)

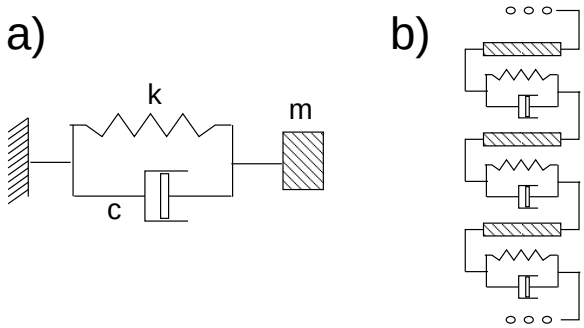

Figure 1. P. Michaels

This is an author-produced, peer-reviewed version of this article. The final, definitive version of this document can be found online at International Journal of Geomechanic, published by American Society of Civil Engineers. Copyright restrictions may apply. doi: 10.1061/(ASCE)1532-3641(2006)6:3(158)

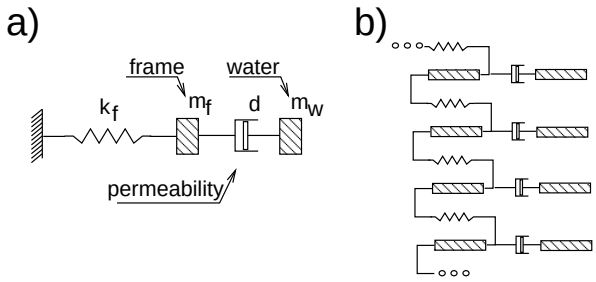

Figure 2. P. Michaels

This is an author-produced, peer-reviewed version of this article. The final, definitive version of this document can be found online at International Journal of Geomechanic, published by American Society of Civil Engineers. Copyright restrictions may apply. doi: 10.1061/(ASCE)1532-3641(2006)6:3(158)

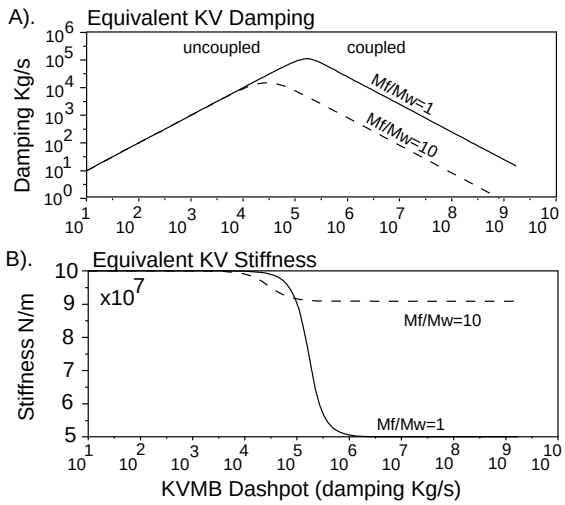

Figure 3. P. Michaels

This is an author-produced, peer-reviewed version of this article. The final, definitive version of this document can be found online at International Journal of Geomechanic, published by American Society of Civil Engineers. Copyright restrictions may apply. doi: 10.1061/(ASCE)1532-3641(2006)6:3(158)

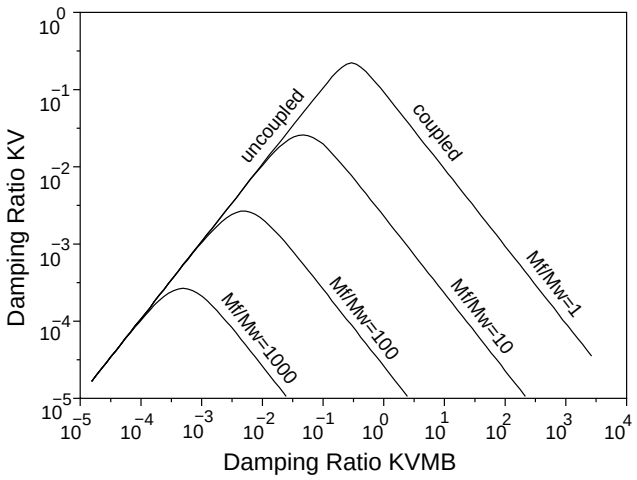

This is an author-produced, peer-reviewed version of this article. The final, definitive version of this document can be found online at International Journal of Geomechanic, published by American Society of Civil Engineers. Copyright restrictions may apply. doi: 10.1061/(ASCE)1532-3641(2006)6:3(158)

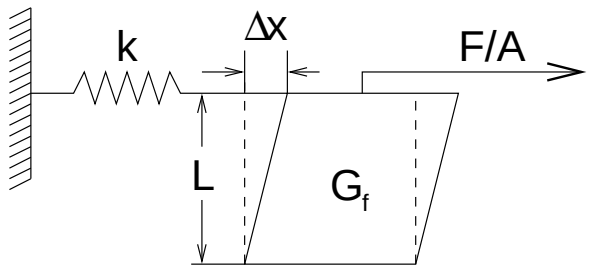

Figure 5. P. Michaels

This is an author-produced, peer-reviewed version of this article. The final, definitive version of this document can be found online at International Journal of Geomechanic, published by American Society of Civil Engineers. Copyright restrictions may apply. doi: 10.1061/(ASCE)1532-3641(2006)6:3(158)

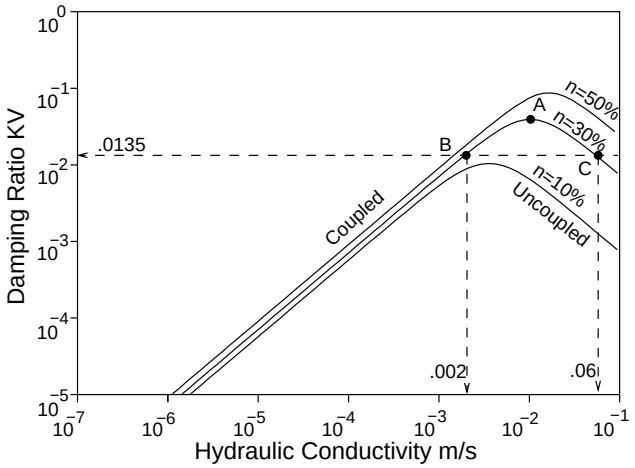

This is an author-produced, peer-reviewed version of this article. The final, definitive version of this document can be found online at International Journal of Geomechanic, published by American Society of Civil Engineers. Copyright restrictions may apply. doi: 10.1061/(ASCE)1532-3641(2006)6:3(158)

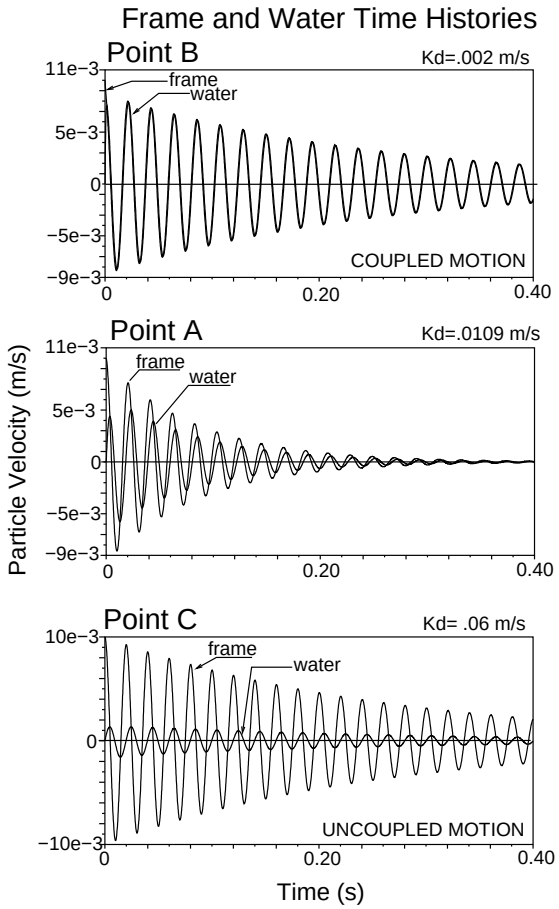

Figure 7. P. Michaels
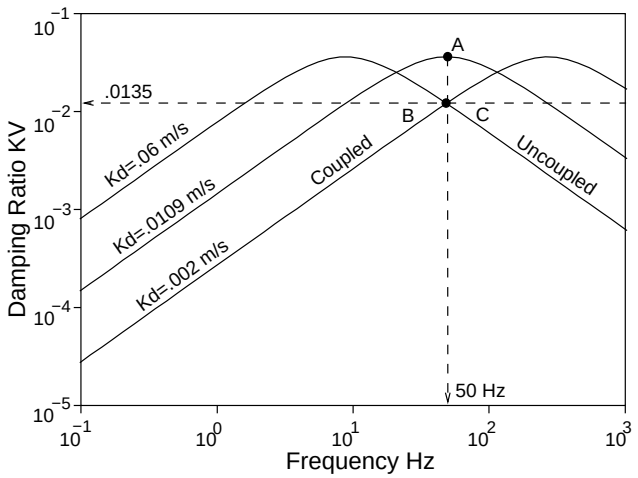
This is an author-produced, peer-reviewed version of this article. The final, definitive version of this document can be found online at International Journal of Geomechanic, published by American Society of Civil Engineers. Copyright restrictions may apply. doi: 10.1061/(ASCE)1532-3641(2006)6:3(158)